JGR Biogeosciences

RESEARCH ARTICLE
10.1029/2020JG006189

Distribution, Source, and Burial of Sedimentary Organic Carbon in Kermadec and Atacama Trenches

Yunping Xu[1], Xinxin Li[2,3], Min Luo[1], Wenjie Xiao[1,2], Jiasong Fang[1], Harunur Rashid[1], Yongbo Peng[4], Wenpeng Li[2], Frank Wenzhöfer[5,6,8], Ashley A. Rowden[7], and Ronnie N. Glud[8,9]

[1]Shanghai Engineering Research Center of Hadal Science & Technology, College of Marine Sciences, Shanghai Ocean University, Shanghai, China, [2]Shenzhen Key Laboratory of Marine Archaea Geo-Omics, Department of Ocean Science and Engineering, Southern University of Science and Technology, Shenzhen, China, [3]Southern Marine Science and Engineering Guangdong Laboratory (Guangzhou), Guangzhou, China, [4]International Center for Isotope Effect Research & School of Earth Sciences and Engineering, Nanjing University, Nanjing, China, [5]HGF-MPG Group for Deep Sea Ecology & Technology, Alfred Wegener Institute Helmholtz Centre for Polar- and Marine Research, Bremerhaven, Germany, [6]Max Planck Institute for Marine Microbiology, Bremen, Germany, [7]Coast and Oceans National Centre, National Institute of Water & Atmosphere Research (NIWA) Ltd, Wellington, New Zealand, [8]Department of Biology, Hadal, Nordcee & DIAS, University of Southern Denmark, Odense M, Denmark, [9]Department of Ocean and Environmental Sciences, Tokyo University of Marine Science and Technology, Tokyo, Japan

Abstract Knowledge of sedimentary organic carbon (OC) in hadal trenches, the deepest ocean realm, is rudimentary. Here, we conducted a comprehensive analysis of total OC (TOC), stable and radio-carbon isotopes ($\delta^{13}C$ and $\Delta^{14}C$), and biomarkers (e.g., *n*-alkanes, *n*-alkanols and *n*-fatty acids) in 12 sediment cores collected from hadal (trench axis) and non-hadal (abyssal plains and slopes) settings of the Kermadec Trench (Southwestern Pacific) and Atacama Trench (Southeastern Pacific) regions. Our results show that the TOC in the Atacama Trench region (0.86% ± 0.69%) is significantly higher than that of the Kermadec Trench region (0.29% ± 0.08%), likely related to different surface primary productivity. In both trench regions, the hadal sites are generally characterized by more negative $\delta^{13}C$, higher TOC/TN ratio, and similar or higher abundance ratio of terrigenous/marine biomarkers as compared to the non-hadal sites, suggesting the selective preservation of terrigenous biogenic/fossil OC at the hadal trench axis. The linear increase in ^{14}C age with sediment depth in non-hadal cores reflects steady depositional conditions, whereas seven out of eight hadal sediment cores show ^{14}C age reversals presumably due to occasional mass-transport deposits. Our results suggest (1) a strong heterogeneity in sedimentary OC characteristics between trenches and within each trench and (2) relatively high accumulation rates of terrigenous OC in both the Kermadec Trench (0.35 ± 0.04 g m^{-2} yr^{-1}) and the Atacama Trench (1.4 ± 0.5 g m^{-2} yr^{-1}). Thus, hadal trenches appear to represent an important environment for terrigenous carbon deposition in the deep ocean.

Plain Language Summary The hadal zone mainly composed of trenches is the deepest ocean realm with water depth over 6,000 m. Due to the challenge of observation and sampling at the extreme depth, the hadal zone is one of the least explored ecosystems on Earth. Limited studies have suggested that hadal trenches have higher benthic biomass and microbial activity compared to surrounding abyssal plains, which has overturned a traditional view that the hadal zone is a "biological desert." Here, we conducted comprehensive geochemical analysis of sedimentary organic carbon in Kermadec Trench (Southwestern Pacific) and Atacama Trench (Southeastern Pacific). Our goal is to understand source, distribution, and burial of organic carbon that is an important food and energy source for benthic organisms in hadal trenches. We have obtained three key findings. (1) While extensive heterogeneity in sedimentary organic carbon in trench interior and between two trenches, the trench bottoms generally have higher fractional abundance of terrigenous organic carbon compared to surrounding abyssal/bathyal sites. (2) Mass-transport deposits induced by episodic events (like earthquakes) profoundly influence organic carbon content and compositions in hadal trenches. (3) The hadal zone is an important but previously overlooked sink for terrigenous organic carbon in the deep ocean.

Yunping Xu, Xinxin Li, and Min Luo contributed equally to this study.

Key Points:

- Sedimentary organic carbon (OC) reflects extensive variations among inter- and intra-trenches
- More terrigenous OC was buried at hadal axis sites compared to non-hadal sites
- The hadal zone is an important and previously overlooked sink for terrigenous OC in deep ocean

Supporting Information:

Supporting Information may be found in the online version of this article.

Correspondence to

Y. Xu and X. Li,
ypxu@shou.edu.cn;
lixinxin@sustech.edu.cn

Citation:

Xu, Y., Li, X., Luo, M., Xiao, W., Fang, J., Rashid, H., et al. (2021). Distribution, source and burial of sedimentary organic carbon in Kermadec and Atacama trenches. *Journal of Geophysical Research: Biogeosciences*, *126*, e2020JG006189. https://doi.org/10.1029/2020JG006189

Received 3 DEC 2020
Accepted 6 APR 2021

Author Contributions:

Conceptualization: Yunping Xu, Ronnie N. Glud
Data curation: Xinxin Li, Wenjie Xiao, Harunur Rashid, Yongbo Peng, Wenpeng Li
Funding acquisition: Yunping Xu, Xinxin Li, Min Luo, Jiasong Fang, Ashley A. Rowden, Ronnie N. Glud
Investigation: Yunping Xu, Xinxin Li, Wenjie Xiao, Wenpeng Li
Methodology: Yunping Xu, Min Luo, Wenjie Xiao, Jiasong Fang, Harunur Rashid, Yongbo Peng, Frank Wenzhöfer, Ronnie N. Glud
Project Administration: Yunping Xu
Resources: Yunping Xu, Frank Wenzhöfer, Ashley A. Rowden, Ronnie N. Glud

Software: Wenjie Xiao, Wenpeng Li
Supervision: Yunping Xu, Xinxin Li
Validation: Min Luo, Yongbo Peng
Writing – original draft: Yunping Xu, Xinxin Li, Min Luo, Ashley A. Rowden, Ronnie N. Glud
Writing – review & editing: Xinxin Li, Min Luo, Jiasong Fang, Harunur Rashid, Frank Wenzhöfer, Ashley A. Rowden, Ronnie N. Glud

1. Introduction

Hadal trenches are located in the subduction zones of the oceans, and represent the deepest (>6 km) and one of the least explored ecosystems on Earth (Jamieson, 2015). Traditionally, the trenches were considered to sustain extremely low biological activities and biomass, but recent studies have demonstrated high abundant biomass of both macrofauna and meiofauna (Danovaro et al., 2002; Itoh et al., 2011), as well as elevated microbial activities in hadal sediments (Glud et al., 2013, 2021; Wenzhöfer et al., 2016) as compared to surrounding abyssal sediments. Such differences have been attributed to sediment focusing and enhanced organic carbon (OC) accumulation at the trench bottom (Jamieson, 2015), a process facilitated by frequent seismic activities, high-frequency fluid dynamics and their V-shaped bathymetry (Bao et al., 2018; Itou et al., 2000; Oguri et al., 2013; Turnewitsch et al., 2014). For example, Kioka et al. (2019) estimated that the giant 2011 Tohoku-Oki earthquake delivered over 1 million tons of OC to the hadal area of the Japan Trench. This type of abrupt OC supply may have a profound influence on the biology and ecology of hadal trenches (Oguri et al., 2013).

Determining the distribution, composition, and source of sedimentary OC is important to understand the cycling and fate of OC in marine sediments (Liu et al., 2013; Meyers, 1997; Niggemann et al., 2007). Bulk geochemical parameters, such as the ratio of total OC (TOC) to total nitrogen (TN) contents (TOC/TN) and stable carbon isotopic composition of TOC ($\delta^{13}C$) have been applied to assess terrigenous versus marine OC in the Puerto Rico Trench (Richardson et al., 1995), the Mariana Trench (Luo et al., 2017), and the New Britain Trench (Luo et al., 2019; Xiao et al., 2020). In addition, radiocarbon composition ($\Delta^{14}C$) of TOC has been used to track the residence time of OC and earthquake-triggered OC burial in the Japan Trench (Bao et al., 2018). Compared to bulk geochemical parameters, molecular biomarkers can provide another dimension of information on specific OC sources (Volkman, 2006). In marine sediments, short-chain ($<C_{20}$) series of *n*-alkanes, *n*-alkanols and *n*-fatty acids are considered as autochthonous marine-derived products (Pancost & Boot, 2004; Volkman et al., 1998), whereas long-chain *n*-alkanes (e.g., $C_{27} + C_{29} + C_{31}$ *n*-alkanes), *n*-fatty acids (e.g., $C_{26} + C_{28} + C_{30}$ *n*-fatty acids), and *n*-alkanols (e.g., $C_{26} + C_{28} + C_{30}$ *n*-alkanols) are primarily derived from allochthonous terrigenous products (Meyers, 1997). A combined application of bulk and molecular parameters provides complementary insights on the composition, source, and degradation stage of OC in marine settings.

In this study, we conducted comprehensive analyses of sedimentary OC at the hadal and non-hadal sites in two contrasting trench systems, namely the Kermadec Trench (KT) and Atacama Trench (AT) regions. The geochemical parameters including the TOC and TN content, TOC/TN ratio, $\delta^{13}C$, $\Delta^{14}C$, and biomarkers were presented and compared. Our major goal is twofold: (1) decipher the distribution, sources, and radiocarbon ages of sedimentary OC in the two trench systems underlying surface water with distinct primary productivity and (2) assess the variability in OC characteristics spanning a wide range of respective trench axis.

2. Material and Methods

2.1. Study Sites

The Kermadec Trench is formed by the subduction of the Pacific Plate underneath the Indo-Australian Plate. It has a maximum water depth of ca. 10,177 m and extends from approximately 26° to 36°S near the North Island of New Zealand (Jamieson, 2015). It is close to the boundary of the deep South Pacific Ocean, and therefore has a deep western boundary current flowing north. This deep current occurs below 2,000 m depth and is the South Pacific component of the global thermohaline circulation, making it an important part of the global climate system (Sutton et al., 2012). While in surface waters, the oceanography is dominated by the South Pacific Subtropical Gyre, an anticlockwise circulation of subtropical water is driven by large-scale winds. Besides these deep and surface currents, internal tide generated along the Kermadec Ridge can make a significant contribution to the global tidal energy dissipation budget, and contribute to sediment focusing or winnowing within the trench interior (Turnewitsch et al., 2014).

During the TAN1711 cruise on RV Tangaroa (November to December 2017), we collected several sediment cores by multiple and box corer sampling. For this study, three cores with intact water-sediment interface

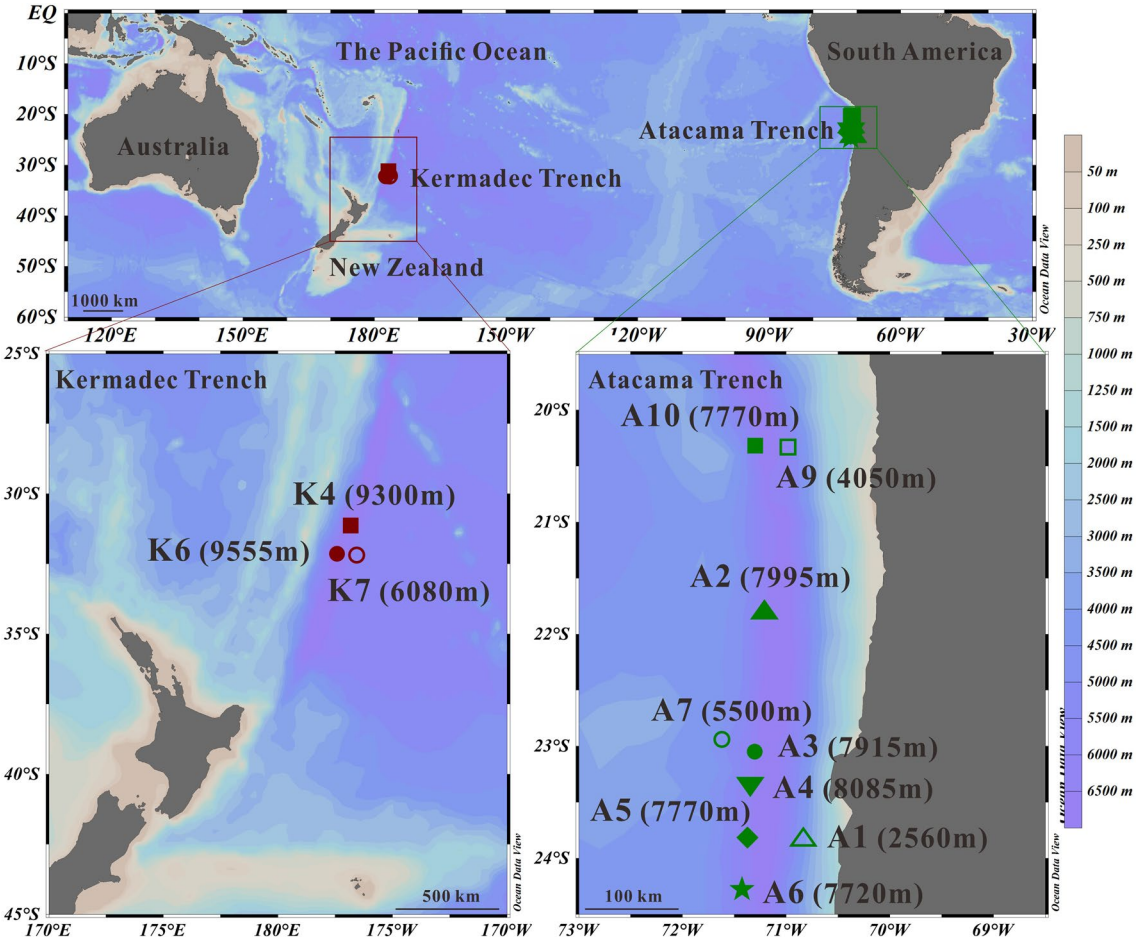

Figure 1. Map showing locations and sampling sites of the Kermadec Trench (K; red) in the southern West Pacific Ocean, and Atacama Trench (A; green) in the southern East Pacific Ocean. Empty and filled symbols denoted non-hadal and hadal sites, respectively (same hereafter).

from three sites were selected for analysis. Two cores were retrieved from the trench axis at water depths of 9,300 (K4) and 9,555 m (K6), and one core (K7) was from the oceanward abyssal plain at a water depth of 6,080 m (Figure 1; Table S1). The sediment cores were sliced on board in 1-cm interval for the top 2 cm sediment, 2-cm interval for 2–10 cm sediment, and 5-cm interval for >10 cm sediment.

The Atacama Trench is the deepest sector of the Peru-Chile Trench that is formed by the subduction of the Nazca Plate underneath the South American Plate (Huene et al., 1999) and has a maximum depth exceeding 8,000 m (Jamieson, 2015). The Peru-Chile Trench is the world's largest trench with a length of 5,900 km and a mean width of 100 km. Due to coastal upwelling, the surface waters offshore Chile-Peru exhibit high primary productivity (Giovanni et al., 2000). Sediment cores were collected during SO261 cruise on RV SONNE in March 2018. A total of nine cores were analyzed, from water depths ranging between 2,560 and 8,085 m (Table S1). One core (A1) was collected from the oceanward abyssal plain, two cores (A7 and A9) from the landward slopes, and six cores (A2, A3, A4, A5, A6, and A10) along the hadal trench axis (Figure 1). Cores were sliced on board at an interval of 1 cm for the top 10 cm sediments, 2.5 cm for 10–20 cm sediments, and 5 cm for >20 cm sediments.

All sediment samples from both the Kermadec and Atacama Trench regions were kept frozen at −20°C until further analysis. Sampling sites were divided into two groups: (1) hadal, from the trench axes having water depths >6,000 m and (2) non-hadal, from abyssal plains (water depths of 4,050–6,080 m) and the landward slope (water depth of 2,560 m).

The data of average net primary productivity (NPP) were downloaded from http://sites.science.oregonstate.edu/ocean.productivity. The NPP was estimated using the Vertically Generalized Production Model (VGPM) based on chlorophyll, available light, and the photosynthetic efficiency (Behrenfeld & Falkowski, 1997). The estimated NPP (January 2009 to December 2018) varied from 144 to 152 g C m^{-2} yr^{-1} in the Kermadec Trench, and from 306 to 449 g C m^{-2} yr^{-1} in the Atacama Trench (Table S1).

2.2. Analytical Methods

2.2.1. Elemental, Stable Carbon and Radiocarbon Isotope Analysis

After being freeze-dried, sediment samples were ground and homogenized with an agate mortar and pestle. Aliquots of dry sediments (2–3 g) were treated with 1 M HCl at room temperature to remove inorganic carbon. Sediments were centrifuged, and the supernatants were gently decanted. After rinsing with ultrapure water, the sediment residues were again freeze-dried and homogenized with the agate mortar and pestle. The TOC and TN contents and $\delta^{13}C$ values were measured by a Vario Pyro Cube elemental analyzer connected to an Isoprime 100 continuous flow isotope ratio mass spectrometer. $\delta^{13}C$ were reported in per mil (‰) using δ notation relative to the Vienna Peedee belemnite standard (V-PDB). The average standard deviation of each measurement, determined by replicate analyses, was ±0.03% for TOC, ±0.02% for TN, and ±0.2‰ for $\delta^{13}C$. The atomic TOC to nitrogen ratio was calculated as: $\mathrm{TOC/TN}\left(\mathrm{mol/mol\ ratio}\right) = \frac{\mathrm{TOC\ content*14}}{\mathrm{TN\ content*12}}$.

The radiocarbon isotope ratios of sedimentary OC was determined using an Accelerator Mass Spectrometry (AMS) at Keck Carbon Cycle Laboratory (University of California, Irvine) (Xu et al., 2007). Radiocarbon data were expressed as $\Delta^{14}C$ values and ^{14}C-AMS ages (Trumbore, 2009). ^{14}C-AMS ages were converted to calendar years before present (BP, relative to CE 1950) using the Calib.7.1 Program with the IntCal13 calibration curve and the global average reservoir age (~400 years) (Reimer et al., 2013).

2.2.2. Lipid Biomarker Analyses

About 2–5 g of the freeze-dried samples was mixed with three internal standards, squalane, C_{19} *n*-fatty acid methyl ester (FAMEs) and C_{19} *n*-alkanol. Sediments were ultrasonically extracted with 15 ml of dichloromethane:methanol (3:1 v/v) for 15 min. The extracts were centrifuged at 3,500 rpm for 10 min, and the supernatants were transferred into pre-combusted glass flasks. This extraction was repeated three times. The combined supernatants were concentrated by a rotary evaporator and dried under N_2 streams. The residues were saponified with 2 mol L^{-1} KOH in methanol at 80°C for 90 min. After the addition of 2 ml ultrapure water, the lipids were extracted with dichloromethane three times. The combined organic phases (neutral fraction) were dried under N_2 streams and derivatized with 30 μl of N, *O*-bis(trimethylsilyl)tri-fluoroacetamide (BSTFA), and 30 μl of pyridine (70°C; 90 min) for *n*-alkanes, *n*-alkanols and sterols analysis. The water phases from saponification containing fatty acids (acid fraction) were acidified to pH < 1 by the addition of 6 mol L^{-1} HCl and then extracted three times by 5 ml of dichloromethane. The organic phase containing fatty acids was blown to dryness under N_2 streams and further derivatized with 1 ml 14% BF_3 in methanol (70°C; 90 min) to form FAMEs. Both neutral and acid fractions were analyzed by an Agilent 7890B gas chromatograph coupled to a 5,975 mass spectrometry (GC-MS) using a capillary column of an Agilent HP-5MS (30 m × 0.32 mm × 0.25 μm). The detailed instrumental capabilities were described by Xu et al. (2018). Biomarkers were identified based on interpretation of mass spectra and comparison with the NIST library. The quantity of *n*-alkanes, *n*-alkanols/sterols, and fatty acids were determined by comparison of total ion chromatogram (TIC) peak areas with internal standards of squalane, C_{19} *n*-alkanol, and C_{19} *n*-FAMEs, respectively.

2.2.3. Data Analysis and Statistics

In order to quantitatively estimate the fractional contribution of marine (F_{marine}) and terrigenous (F_{terr}) organic matter to the sedimentary OC pool, a two-endmember mixing model was applied based on $\delta^{13}C$ (or TOC/TN). Since terrigenous organic matter is relatively depleted in nitrogen (with high atomic TOC/TN ratios of 20–160), the fraction of terrigenous derived OC can be systematically underestimated given a non-linear relation between the TOC/TN ratio and F_{terr} in the two-endmember mixing equation. As a result,

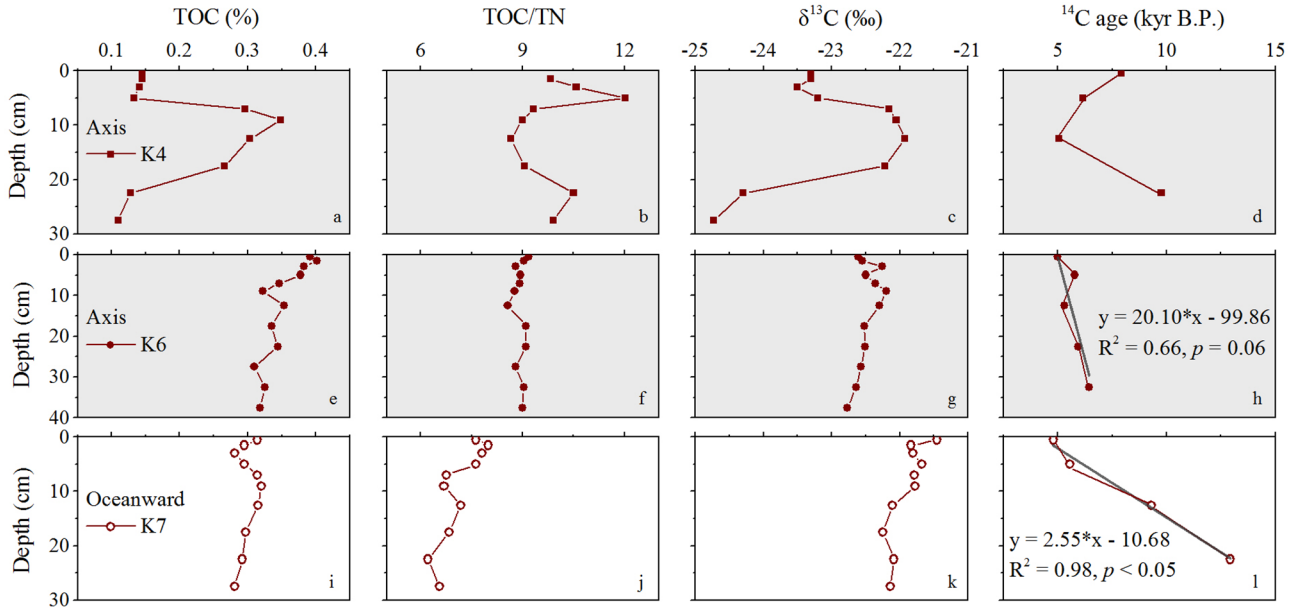

Figure 2. Depth profiles of TOC, TOC/TN (mol/mol ratio), $\delta^{13}C$, and ^{14}C ages of sedimentary organic matter in three cores (K4, K6, and K7) from the Kermadec Trench region. TOC, total organic carbon; TN/TOC, total organic/total nitrogen contents.

Perdue and Koprivnjak (2007) recommended the use of TN/TOC ratio to yield the desirable result about F_{terr}. Here, the F_{terr} and F_{marine} were calculated as follows.

$$\delta^{13}C_{sample} = F_{marine} \times \delta^{13}C_{marine} + F_{terr} \times \delta^{13}C_{terr}$$

$$\left(TN / TOC\right)_{sample} = F_{marine} \times \left(TN / TOC\right)_{marine} + F_{terr} \times \left(TN / TOC\right)_{terr}$$

$$F_{terr} = 1 - F_{marine}$$

For the Kermadec Trench, the $\delta^{13}C$ was assigned as −21.0‰ for the marine endmember value based on southern ocean phytoplankton (Popp et al., 1999) and −25.8‰ for the terrigenous endmember value based on riverine particulate OC in New Zealand (Leithold et al., 2006). For the Atacama Trench region, the $\delta^{13}C$ was assigned as −20.2‰ for the marine endmember value based on suspended particulate OC of Peruvian upwelling regions (Pancost et al., 1999) and −26.5‰ for the terrigenous endmember value based on the riverine particulate organic carbon in central Chile (Vargas et al., 2013). For the TOC/TN ratio, terrigenous plants have a typical value of 20 and greater, whereas marine algae have the value between 4 and 10 (Meyers, 1997). In our study, the TOC/TN ratio was assigned as 50 for the terrigenous endmember value and 6.0 for the marine endmember value (Li et al., 2020; Perdue & Koprivnjak, 2007). The corresponding TN/TOC ratios of terrigenous and marine endmembers are 0.02 and 0.17, respectively.

The software package SPSS 22 (IBM) was used for statistical analyses. One-way analysis of variance (ANOVA) and principal component analysis (PCA) were performed for different sites based on various parameters (e.g., TOC, $\delta^{13}C$, TOC/TN, and biomarkers). The significant level was set at $p < 0.05$.

3. Results

3.1. Bulk Geochemical Parameters of Sedimentary OC in the Kermadec Trench Region

The two hadal sites in the Kermadec Trench (K4 and K6) showed somewhat contrasting trends in bulk geochemical parameters (Figures 2a–2h). Significant changes in bulk carbon parameters occurred at 5–15 cm depths of the core K4, exhibited by higher TOC contents (>0.2%), lower TOC/TN ratios (<9.5), less negative $\delta^{13}C$ (>−22.5‰) and younger ^{14}C ages (<6.5 kyr BP) (Figures 2a–2d) than the rest of the cores. One possible

Table 1
Bulk Geochemical Parameters and Terrigenous/Marine Biomarker Ratio in Sediment Cores of Atacama Trench (A) and Kermadec Trench (K)

	Site	TOC (%)	TOC/TN (mol/mol)	$\delta^{13}C$ (‰)	^{14}C age (kyr BP)	Terrigenous/marine biomarkers*
K7	Oceanward abyssal	0.30 ± 0.01	7.1 ± 0.6	−21.9 ± 0.2	4.79~12.93	0.058 ± 0.019
K4	Hadal	0.21 ± 0.09	9.9 ± 1.0	−23.1 ± 0.9	5.07~9.76	0.022 ± 0.008
K6	Hadal	0.35 ± 0.03	8.9 ± 0.2	−22.5 ± 0.2	5.01~6.45	0.12 ± 0.18
A1	Landward slope	2.28 ± 0.55	7.7 ± 0.8	−21.3 ± 0.2	2.43~5.23	0.43 ± 0.15
A9	Landward abyssal	1.12 ± 0.18	7.5 ± 0.7	−21.5 ± 0.2	3.09~13.43	0.70 ± 0.30
A7	Oceanward abyssal	0.39 ± 0.13	7.0 ± 0.4	−20.9 ± 0.3	3.24~28.6	0.57 ± 0.21
A2	Hadal	0.59 ± 0.22	9.7 ± 0.5	−22.2 ± 0.3	4.19~9.11	0.39 ± 0.17
A3	Hadal	0.44 ± 0.05	12.1 ± 0.9	−23.7 ± 0.7	8.26~21.40	0.56 ± 0.30
A4	Hadal	0.42 ± 0.07	8.7 ± 0.4	−22.7 ± 0.3	5.96~8.94	1.18 ± 0.40
A5	Hadal	0.48 ± 0.09	8.7 ± 0.9	−22.4 ± 0.3	4.58~10.63	0.81 ± 0.33
A6	Hadal	0.44 ± 0.08	8.5 ± 0.8	−23.5 ± 0.4	4.89~8.94	1.36 ± 0.54
A10	Hadal	1.49 ± 0.38	9.4 ± 0.1	−21.7 ± 0.3	2.99~4.14	0.69 ± 0.18

Note. terrigenous/marine biomarkers denote the abundance ratio of
$$\frac{C27 + C29 + C31\,n-\text{alkanes} + C26 + C28 + C30\,n-\text{alkanols} + C26 + C28 + C30\,n-\text{fatty acids}}{C17 + C19 + C21\,n-\text{alkanes} + C14 + C16 + C18\,n-\text{alkanols} + C14 + C16 + C18\,n-\text{fatty acids}}.$$
Abbreviations: OC, organic carbon; TerrOC, terrigenous organic carbon; TOC, total organic carbon; TN, total nitrogen.

explanation could be downslope mass wasting event from trench flanks or from the abyssal plain toward the trench axis. In contrast, the hadal site (core K6) did not show dramatic depth variations for bulk geochemical parameters, but merely a gradual downcore decline in values of TOC and $\delta^{13}C$ (Figures 2e–2h).

At the hadal site K4, the average TOC (%), TOC/TN and $\delta^{13}C$ were 0.21% ± 0.09% (Mean ± SD, same hereafter), 9.87 ± 0.99, and −23.1‰ ± 0.9‰, respectively (Table 1). The measured ^{14}C ages of TOC for 0–1, 4–6, 10–15 and 20–25 cm sediments varied between 5.1 and 9.8 kyr BP. At the hadal site K6, the average TOC, TOC/TN, and $\delta^{13}C$ were 0.35% ± 0.03%, 8.93 ± 0.17, and −22.5‰ ± 0.2‰, respectively (Table 1). The ^{14}C ages of TOC in core K6 varied in a narrower range (5.0–6.5 kyr BP) relative to that in core K4, and displayed an increasing trend with depth ($R^2 = 0.66$; $p = 0.06$), allowing an estimation of the sedimentation rate of 20.1 cm kyr^{-1} (Figure 2h).

The oceanward abyssal site (K7) was characterized by little depth variations in bulk geochemical parameters when compared to the hadal site K4 (Figures 2i–2k). At site K7, the average TOC (%), TOC/TN, and $\delta^{13}C$ were 0.30% ± 0.01%, 7.13 ± 0.57, and −21.9‰ ± 0.2‰, respectively (Table 1). Both TOC/TN and $\delta^{13}C$ value showed an apparent downcore decline (Figures 2j and 2k), whereas the ^{14}C ages of TOC exhibited a linear increase with depths ($R^2 = 0.98$; $p < 0.05$), suggesting a mean sedimentation rate of 2.55 cm kyr^{-1} that was significantly lower than that at the trench axis site of K6 (Figure 2l).

Compared to the non-hadal site (K7), the hadal sites (K4, K6) had similar TOC (0.28% ± 0.10% vs. 0.30% ± 0.01%; $p = 0.94$), but significantly higher TOC/TN (9.34% ± 0.81% vs. 7.13% ± 0.57%; $p < 0.001$) and more negative $\delta^{13}C$ values (−22.8‰ ± 0.7‰ vs. −21.9‰ ± 0.2‰; $p < 0.01$).

3.2. Bulk Geochemical Parameters of Sedimentary OC in the Atacama Trench Region

In the Atacama Trench, the depth profiles of TOC, TOC/TN, and $\delta^{13}C$ at the hadal sites (A2, A3, A4, A5, A6, and A10) generally showed larger variability as compared to non-hadal sites (A1, A7, and A9) (Figure 3). The ^{14}C ages of TOC exhibited positive linear correlations with sediment depths at three non-hadal sites ($R^2 = 0.83$ to 0.99; $p \leq 0.06$), suggesting steady depositional conditions with a sedimentation rate of 6.32 (A1), 0.81 (A7), and 1.23 cm kyr^{-1} (A9), respectively (Figure 3). In contrast, all sediment cores at the hadal

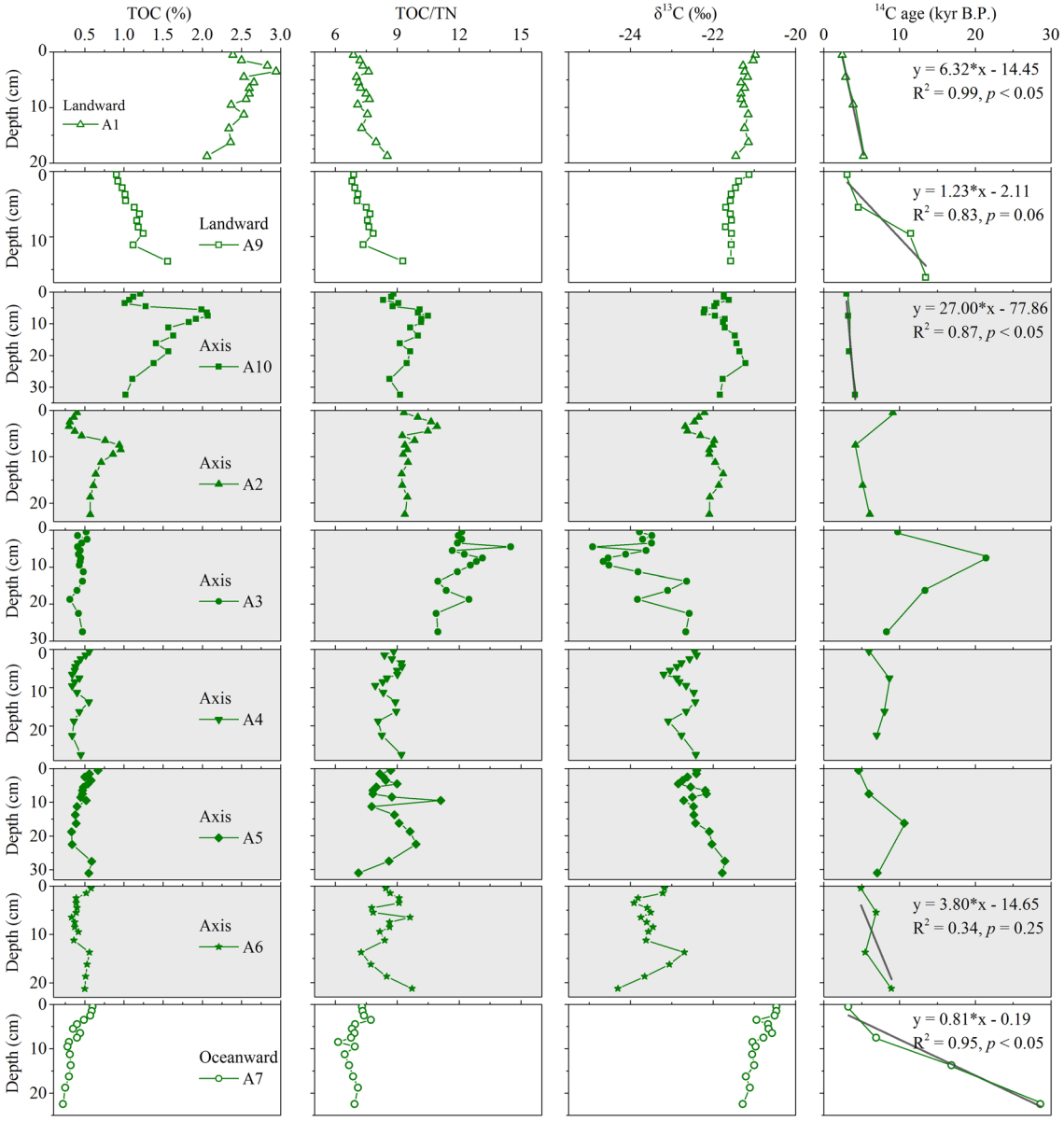

Figure 3. Depth profiles of TOC, TOC/TN, $\delta^{13}C$ and ^{14}C ages of sedimentary organic matter in nine cores from the Atacama Trench region (A), including one core from landward slope site (A1), one core from landward abyssal site (A9), six cores from hadal trench sites (A2, A3, A4, A5, A6, and A10) and one core from oceanward abyssal site (A7). TOC, total organic carbon; TN/TOC, total organic/total nitrogen contents.

axis sites except A10 showed apparent ^{14}C age reversals (A2, A3, A4, A5, and A6; Figure 3), indicating disturbed sediment deposition conditions. Although one hadal site (A10) showed an increasing trend of the ^{14}C age with sediment depth ($R^2 = 0.87$; $p < 0.05$; Figure 3), its sedimentation rate (27.0 cm kyr^{-1}) was significantly higher than that at the non-hadal sites. Additionally, the depth profiles of the TOC, TOC/TN and $\delta^{13}C$ in core A10 displayed large variations in the upper 10 cm, suggesting an unstable depositional condition.

In the Atacama Trench region, the average value of TOC, TOC/TN, and $\delta^{13}C$ was 0.86% ± 0.69%, 8.84 ± 1.60, and −22.2‰ ± 1.0‰, respectively. Across the trench region, sedimentary TOC varied considerably, with an average of landward non-hadal sites (A1 and A9; 1.87% ± 0.72%) > hadal axis sites (A2, A3, A4, A5, A6, and A10; 0.65% ± 0.43%) > oceanward non-hadal site (A7; 0.39% ± 0.13%) (Figure 4a). Correspondingly, the TOC/TN was the highest at the hadal axis (9.51 ± 1.42), followed by the landward sites (7.45 ± 0.53) and then the oceanward site (6.95 ± 0.38) (Figure 4b), whereas the $\delta^{13}C$ values gradually increased in the order

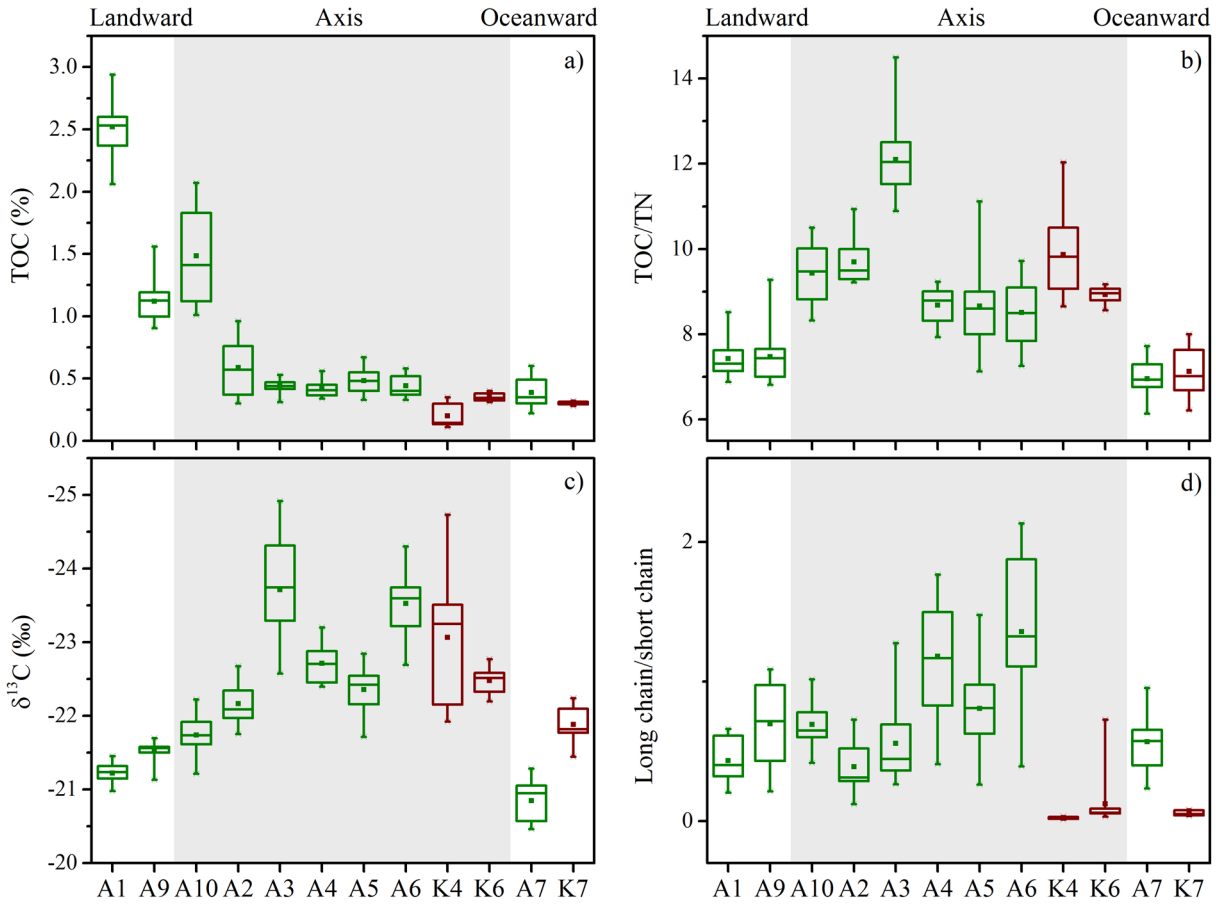

Figure 4. Box plots of TOC (a), TOC/TN (b), $\delta^{13}C$ (c), and terrigenous/marine biomarker ratio (d) in sediment cores from Kermadec Trench (K) and Atacama Trench (A) regions. The parameters from bottom to the top of the boxplots present the lower extreme, lower quartile, median, average, upper quartile, and upper extreme values, respectively. TOC, total organic carbon; TN/TOC, total organic/total nitrogen contents.

of the hadal axis (−22.7‰ ± 0.8‰), the landward sites (−21.4‰ ± 0.2‰) and the oceanward abyssal site (−20.9‰ ± 0.3‰) (Figure 4c).

3.3. Biomarkers in the Kermadec Trench and Atacama Trench

Homologs of *n*-alkanes ($C_{16} \sim C_{31}$), *n*-alkanols ($C_{18} \sim C_{30}$) and *n*-fatty acids ($C_{14} \sim C_{32}$) were quantified in Kermadec and Atacama Trench sediments (Supplementary material) and used to distinguish between different sources of the organic matter. Long chain homologs of $C_{27} + C_{29} + C_{31}$ *n*-alkanes, $C_{26} + C_{28} + C_{30}$ *n*-alkanols and $C_{26} + C_{28} + C_{30}$ *n*-fatty acids were terrigenous biomarkers, whereas short-chain homologs of $C_{17} + C_{19} + C_{21}$ *n*-alkanes, $C_{14} + C_{16} + C_{18}$ *n*-alkanols and $C_{14} + C_{16} + C_{18}$ *n*-fatty acids were marine biomarkers (Meyers, 1997). Given large amplitude variability of individual biomarker abundance in each core and the potentially different dilution effects at different sites, an abundance ratio of long chain/short chain *n*-alkanes + *n*-alkanols + *n*-fatty acids (termed as terrigenous/marine biomarkers) was taken to assess the relative importance of terrigenous and marine OC.

Along the Kermadec Trench axis, the mean value of terrigenous/marine biomarker ratio was 0.022 ± 0.008 in core K4 and 0.12 ± 0.18 in core K6, respectively (Table 1). At the abyssal site of the Kermadec Trench (K7), the mean value of terrigenous/marine biomarker ratio was 0.058 ± 0.019. Overall, there were no significant differences between the hadal sites and non-hadal site in the Kermadec Trench ($p > 0.05$), highlighting the intra-trench heterogeneity in biomarker distributions (Figure 4d).

In the Atacama Trench region, the mean value of terrigenous/marine biomarker ratio at the six hadal sites was 0.39 ± 0.17 in core A2, 0.56 ± 0.30 in core A3, 1.18 ± 0.40 in core A4, 0.81 ± 0.33 in core A5, 1.36 ± 0.54 in core A6, and 0.69 ± 0.18 in core A10 (Table 1). For three non-hadal sites, the terrigenous/marine biomarker ratio had a value of 0.43 ± 0.15 in core A1, 0.57 ± 0.21 in core A7, and 0.70 ± 0.30 in core A9. Taken together, the mean value of terrigenous/marine biomarker ratio was 0.84 ± 0.47 at the hadal sites, significantly higher than that at the non-hadal sites (0.56 ± 0.24) ($p < 0.01$). However, the prominent heterogeneity exists among the trench axis sites, such as higher terrigenous/marine biomarker ratio at sites A4 and A6 as compared to sites A2, A3, A5, and A10 ($p < 0.001$; Figure 4d).

4. Discussion

4.1. Composition and Distribution of Sedimentary OC in the Kermadec and Atacama Trench

Hadal trenches have been proposed as deep sea depocenters for OC, reflected by higher sedimentary TOC content at trench axes than adjacent abyssal plains, for example, in the Atacama Trench region (Danovaro et al., 2003), the Mariana Trench region (Glud et al., 2013), the New Britain Trench region (Xiao et al., 2020), and the Yap Trench (Li et al., 2020). This is likely explained by downward sediment transport processes (e.g., mass wasting deposition events) along the trench flanks and material focusing effects at the trench axis (Bao et al., 2018; Wenzhöfer et al., 2016). As a result, the average TOC contents at the axes of both the Kermadec and Atacama Trench regions are generally higher than those at the adjacent oceanward abyssal sites (Figure 4a). However, regional differences along the investigated trench axes can be observed. The slightly lower TOC content at the hadal site K4 may be related to translocation of OC-depleted sediments from shallower site to the trench axis as compared to the abyssal site K7 (Figure 4a). This is further supported by the older ^{14}C ages of TOC in core K4 relative to core K6 (Figures 2d and 2h). In the Atacama Trench, apparent higher TOC content was found at site A10 as compared to sites A2, A3, A4, A5, and A6, although they were all taken from the hadal axis (Figure 4a). These differences highlight the heterogeneity of sedimentary TOC along the trench axis due to complex environmental processes including turbidity currents that are triggered by earthquakes, rapidly transporting sediments from shallow water into the hadal trenches (Bao et al., 2018; Itou et al., 2000), internal tides that might drive winnowing or focusing of vertical material supply (Turnewitsch et al., 2014), and the complex topography within the interior trench such as local ponds and escarpments (Stewart & Jamieson, 2018).

Sedimentary OC in trenches can be a mixture of autochthonous marine-derived OC mainly from surface primary production and allochthonous terrigenous OC mainly derived from adjacent continents (Gallo et al., 2015; Luo et al., 2019; Xiao et al., 2020). It has been hypothesized that settling of diatom detritus facilitated rapid hadal deposition of short-lived ^{134}Cs released from the Fukushima nuclear power plant following the Tohoku-Oki earthquake and tsunami in 2011 (Oguri et al., 2013). This highlights the important linkages between primary productivity and hadal OC deposition and burial, which well explains the overall higher TOC content in the Atacama Trench underlying the eutrophic waters as compared to that in the Kermadec Trench underlying the mesotrophic waters (Figure 4a). Therefore, inter-trench heterogeneity in sedimentary TOC content appears to be related to the regional surface ocean productivity, but other factors may modulate the spatial variability of sedimentary OC content at intra-trench scale.

The accumulation of terrigenous OC in trench systems has been ascribed to lateral transport from adjacent lands and coastal waters (Baudin et al., 2017; de Stigter et al., 2007; Leduc & Rowden, 2018; Luo et al., 2019; Xiao et al., 2020). In the Kermadec and Tonga Trench regions, the surface sediments exhibit substantially higher pollen biomasses at hadal sites (>7,000 m) relative to non-hadal sites (Leduc & Rowden, 2018). While in the New Britain Shelf-Trench continuum, the efficient sequestration of terrigenous OC in the hadal environment is evidenced from bulk and molecular geochemistry such as TOC content, TOC/TN, $\Delta^{14}C$, $\delta^{13}C$, and fatty acids (Luo et al., 2019; Xiao et al., 2020). In this study, higher TOC/TN and more negative $\delta^{13}C$ values were generally exhibited at the hadal sites along the axes of the Kermadec and Atacama trenches, whereas sediments at the non-hadal sites have lower TOC/TN and less negative $\delta^{13}C$ values, suggesting an increase in the fraction of terrigenous OC along the hadal axes of both trenches (Figure 5a). A significant linear correlation between TOC and TN ($R^2 = 0.97$; $p < 0.005$; Figure 5b) suggests that nitrogen in the sediment is primarily associated with organic matter. Most of the samples at the non-hadal sites are located above the regression line, while those at the hadal sites are below the regression line (Figure 5b). Therefore,

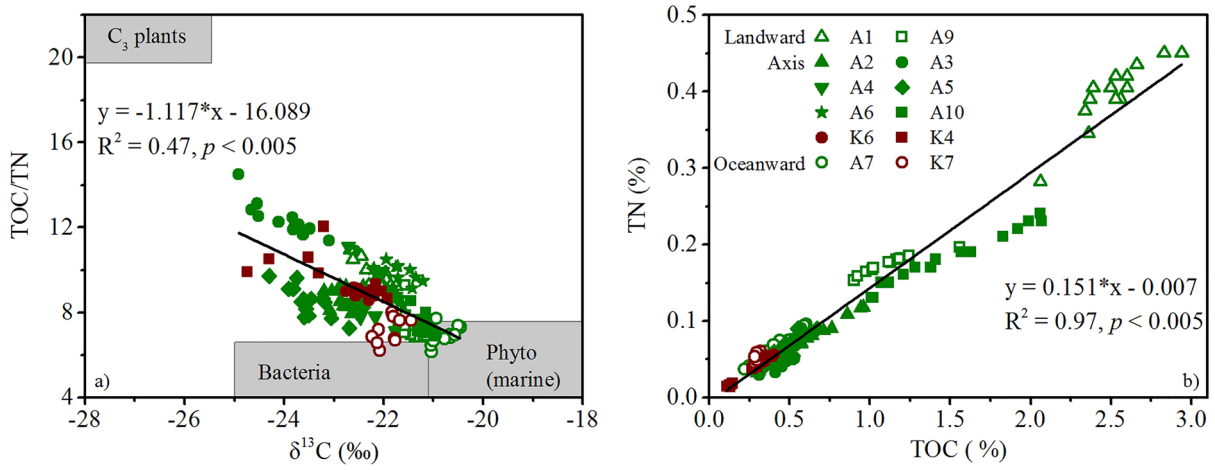

Figure 5. Correlations between geochemical parameters in sediments of Kermadec (K) and Atacama (A) trench regions. (a) TOC/TN versus $\delta^{13}C$, and (b) TN versus TOC. TOC, total organic carbon; TN/TOC, total organic/total nitrogen contents.

sedimentary OC at hadal sites on average contained more N-depleted and presumably terrigenous compounds (e.g., cellulose, lignin, and lipid) compared to more N-enriched marine compounds (e.g., protein) at the non-hadal sites, again suggesting the enrichment of terrigenous OC at the hadal axes.

4.2. Quantification of Terrigenous and Marine Derived OC in the Kermadec and Atacama Trench

The source apportionment of OC in marine sediments is challenging given multiple sources and complex environmental processes. However, our two-endmember mixing model using $\delta^{13}C$ and TN/TOC ratio yielded similar results about fractional abundance of terrigenous OC (F_{terr}) and marine OC (F_{mar}) (Figures 6a, and 6b), reflected by a significant positive correlation ($r = 0.68$, $p < 0.005$; Figure 6c). The mean F_{terr} and F_{mar} based on the $\delta^{13}C$ was 31% ± 15% and 69% ± 15%, respectively, in the Kermadec Trench, and 32% ± 16% and 68% ± 16%, respectively, in the Atacama Trench. Based on the TN/TOC ratio, the mean F_{terr} and F_{mar} was 33% ± 13% and 67% ± 13%, respectively, in the Kermadec Trench and 34% ± 13% and 66% ± 13%, respectively, in the Atacama Trench. Considering the consistent results derived from $\delta^{13}C$ and TN/TOC ratio, we only discuss the $\delta^{13}C$-based F_{terr} hereafter.

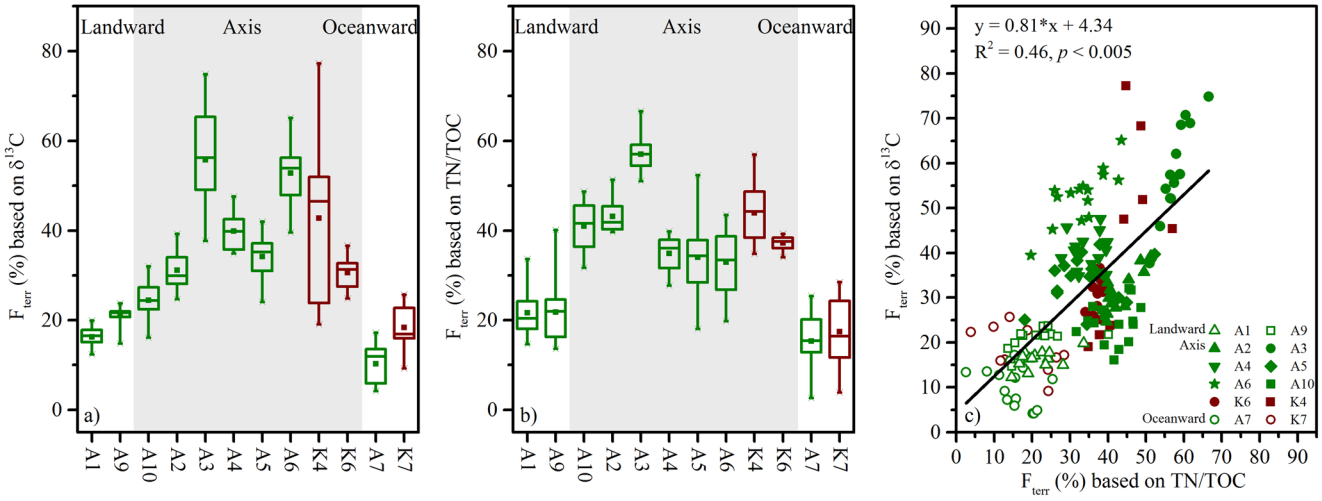

Figure 6. The proportion of terrigenous OC (F_{terr}) based on $\delta^{13}C$ (a) and TN/TOC ratio (b) according to the two-endmember mixing model; and the correlation of F_{terr} between the $\delta^{13}C$ and TN/TOC ratio (c). OC, organic carbon; TN/TOC, total organic/total nitrogen contents.

In the Kermadec Trench, the fractional abundance of terrigenous OC (F_{terr}) at the trench axis sites (K4 and K6; 36% ± 15%) was 18% higher than that at the oceanward abyssal site K7 (18% ± 5%). Similarly, in the Atacama Trench, the mean F_{terr} at the six trench axis sites (40% ± 16%, A2, A3, A4, A5, A6, and A10) in the Atacama Trench was about 24% higher than that at the three non-hadal sites (16% ± 5% at A1, A7, and A9). The F_{terr} at trench axis site A10 (24% ± 4%) was even 3% higher than the adjacent landward slope site A9 (21% ± 2%), although the site A9 is closer to the landmass (Figure 1). The higher terrigenous/marine biomarker ratio at the hadal sites of the Atacama Trench also supports an enrichment of terrigenous OC at the trench axis (Figure 4d). Generally, such high F_{terr} is unexpected, especially for the hadal sites in the Kermadec Trench that are almost 700 km away from the adjacent landmass. This can be explained by a lateral transport of terrigenous OC from shelves/continental slopes to the hadal sites and better preservation of terrigenous OC relative to marine OC during the transport. It is well known that the terrigenous OC is more refractory compared to marine OC (Burdige, 2007). Thus, during the transport to the hadal settings, marine-derived OC was preferentially degraded, leading to the relative enrichment of terrigenous OC. This hypothesis is supported by the higher pollen abundance in hadal sediments relative to non-hadal sediments in the Kermadec and Tonga trenches (Leduc & Rowden, 2018), and higher soil microbial biomarkers at the hadal sites compared with non-hadal sites in the Kermadec and Atacama Trenches (Xu et al., 2020). A recent study based on in-situ measurement in Kermadec and Atacama trench regions suggested that benthic oxygen consumption at all hadal sites was intensified relative to adjacent abyssal plains, highlighting that hadal trenches represent deep sea hotspots for early diagenesis (Glud et al., 2021). Under this condition, marine OC that is presumably more labile compared to terrigenous OC was selectively degraded in the trench sediments, further contributing to the enrichment of terrigenous OC at the trench bottom.

Terrigenous OC can be further separated into biogenic (recently photosynthesized) and fossil (ancient combusted) carbon. It has been found that the concentration of fossil carbon (i.e., graphitic black carbon) increases roughly linearly with increasing distance offshore, reaching 6.5% of TOC in marine sediments at 200 km distance offshore at the Washington Coast (Dickens et al., 2004). If this linear correlation is extrapolated to the Kermadec trench, the fractional contribution of graphitic black carbon would be up to 20% of the TOC, which may help to explain the high F_{terr} along the trench axis. However, the lack of significant differences in terrigenous/marine biomarker ratio between hadal and non-hadal sites of the Kermadec Trench (Figure 4d) suggests the complex OC sources and heterogenous OC compositions within the trench interior. Since the lipid biomarker approach is unable to characterize fossil carbon, it may underestimate the contribution of total terrigenous OC. Thus, the investigation for more specific terrigenous biomarkers (e.g., lignin for vascular plants or BPCA for black carbon) (Brodowski et al., 2005; Hu et al., 1999) is needed in future studies.

4.3. ^{14}C Age of Sedimentary OC in the Kermadec and Atacama Trench

For both Kermadec and Atacama Trench regions, the sedimentary OC from hadal and non-hadal sites exhibits heterogenous ^{14}C ages (Figure 4b), which can be explained by different sources of the settling OC with distinct Δ^{14}C (i.e., marine OC, terrigenous biogenic, and fossil OC) and different degradation stages (Eglinton et al., 1997). Sedimentary OC at the non-hadal sites (K7, A1, A7, and A9) showed less negative δ^{13}C values and lower TOC/TN ratios (Figures 4b and 4c), suggesting the predominance of marine-derived OC. In contrast to the non-hadal sites, the hadal sites (K4, K6, A2, A3, A4, A5, A6, and A10) generally show more negative δ^{13}C, higher TOC/TN and higher terrigenous/marine biomarker ratio (Figures 4b–4d), suggesting higher fractional abundance of terrigenous-derived OC. The TOC content and Δ^{14}C varied greatly among different sites, but in general, sediments containing lower TOC (<1% at K4, K6, K7, A2, A3 A4, A5, A6, and A7) show an older and more variable Δ^{14}C values (between −1,000‰ and −400‰), whereas sediments characterized by higher TOC contents (>1% at A1, A9, and A10) exhibit younger and relatively constant Δ^{14}C values (between −400‰ and −300‰) (Figure 7a). This again points to a considerable spatial variability in sedimentary OC along the investigated trench transects. The Δ^{14}C values show a significant linear correlation with δ^{13}C for the hadal sediments ($R^2 = 0.50$; $p < 0.005$), whereas no significant correlation exists for the non-hadal sediments ($R^2 = 0.06$; $p = 0.19$) (Figure 7b). Different sources of OC and environmental processes are responsible for the ^{14}C ages of the settling OC between hadal and non-hadal sediments. At the non-hadal sites (abyssal plains/landward slopes), sedimentary OC generally reveal narrower and less negative δ^{13}C values (−21.3‰ ± 0.4‰; Figure 4c), suggesting a predominance of marine OC source. Thus,

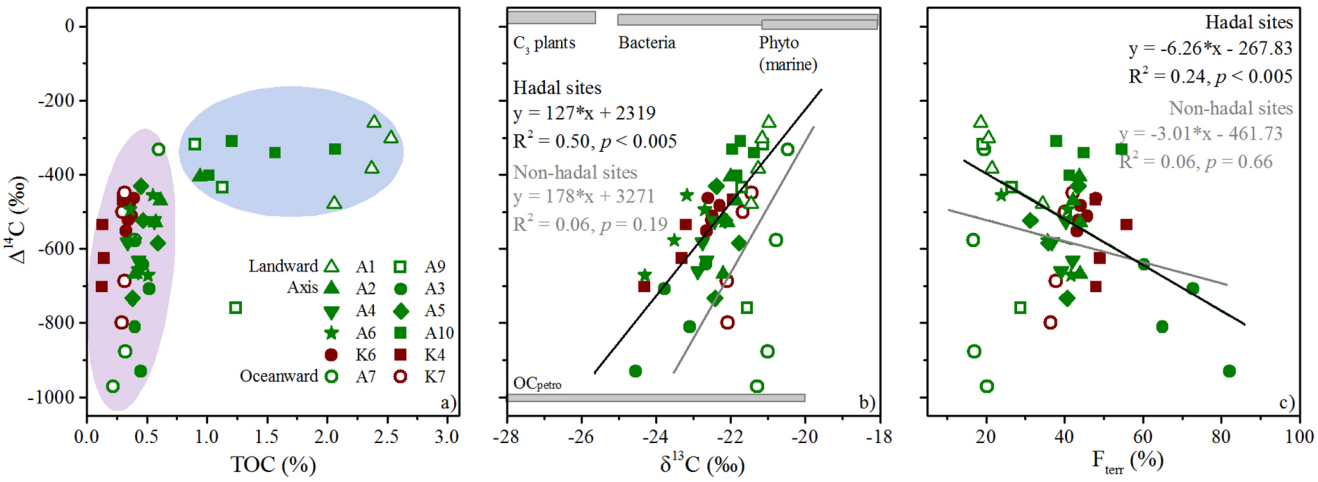

Figure 7. Relationships of $\Delta^{14}C$ of OC with (a) TOC; (b) $\delta^{13}C$ and (c) fraction of terrigenous OC (F_{terr}) in sediments of Kermadec (K) and Atacama (A) trench regions. TOC, total organic carbon.

the ^{14}C ages in non-hadal cores are mainly controlled by post-depositional decay of marine OC. In contrast, at the hadal sites (trench axes), sedimentary OC is characterized by more negative and larger variable $\delta^{13}C$ values (−22.7‰ ± 0.8‰; Figure 4c), suggesting different contributions of terrigenous and marine-derived OC to the hadal sedimentary OC pool (Figure 7c). Consequently, the geochemical characteristics of sedimentary OC (e.g., TOC contents, $\Delta^{14}C$, and $\delta^{13}C$) across the trenches are influenced by source variability and post-depositional processes to different degrees. At the hadal sites, variable contributions from two source endmembers play a key role in controlling sedimentary TOC contents and carbon isotopic compositions: (1) marine OC from recent photosynthesis in the surface ocean and characterized by higher $\Delta^{14}C$ (young radiocarbon age) and less negative $\delta^{13}C$ values and (2) terrigenous OC (including biogenic and fossil OC), characterized by lower $\Delta^{14}C$ (old radiocarbon age) and more negative $\delta^{13}C$, derived from pre-aged soil carbon or ^{14}C-dead petrogenic carbon from bedrocks (French et al., 2018; Valier et al., 2015). An additional factor for OC aging is long-distant transport of terrigenous OC from interior land to the trench axes.

The degradation of OC is closely linked to depositional conditions such as bioturbation and physical mixing (Niggemann et al., 2007) and episodic events such as submarine landslides (Bao et al., 2018). The ^{14}C ages of TOC at the non-hadal sites (K7, A1, A7, and A9) generally increase linearly with sediment depth (Figures 2 and 3), indicating steady depositional conditions with relatively low sedimentation rates (0.83–2.55 cm kyr^{-1}). Slightly negative shifts in $\delta^{13}C$ values deeper in the cores (Figures 2 and 3) reflect a typical post-depositional decay of marine OC (Henrichs, 1992; Prahl et al., 1997), which results in a decrease of $\delta^{13}C$ and an increase of TOC/TN. In contrast, the hadal sediment cores showed disturbed depositional conditions, leading to reversed trends of ^{14}C ages (i.e., K4, K6, A2, A3, A4, A5, and A6) and abrupt changes in TOC, TOC/TN, and $\delta^{13}C$ values (Figures 2 and 3). Frequent sea-bed instability and the steep trench slope could induce sediment remobilization and downslope sediment transport of OC to the hadal environments (Bao et al., 2018; Ichino et al., 2015; Kioka et al., 2019). Consequently, unlike surrounding abyssal plains and landward slopes, the relatively continuous steady deposition at the trench axis was overlaid by rapid accumulation of sediment and OC with different ^{14}C ages, thus leading to distinct vertical variations in geochemical features of the deposited OC.

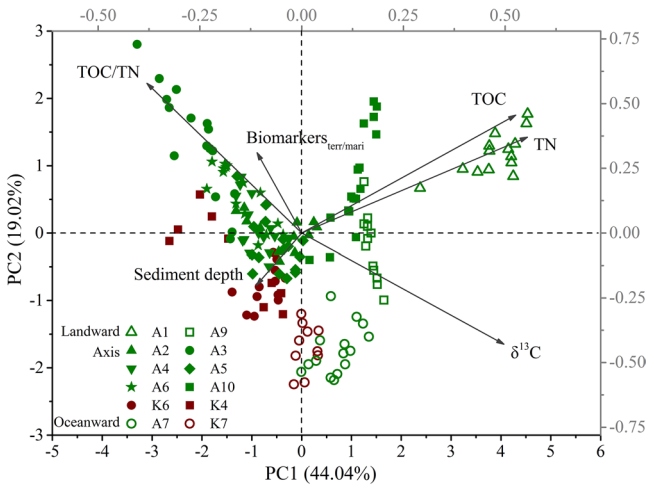

Figure 8. Principal component analysis based on bulk and molecular parameters in sediment cores taken from Kermadec (K) and Atacama (A) trench regions.

The principal component analysis based on bulk and molecular parameters separated hadal and nonhadal sediment samples (Figure 8). The first principal component (PC1) and second principal component (PC2)

Table 2
Estimated OC and TerrOC Accumulation Rates in the Kermadec Trench and Atacama Trench

	Kermadec (core K6)	Atacama (core A10)
TOC (%)	0.31~0.40	1.01~2.07
F_{terr} based on $\delta^{13}C$ (%)	25~36	16~32
OC accumulation rate (g m^{-2} yr^{-1})	0.94 ± 0.08	5.6 ± 1.4
TerrOC accumulation rate (g m^{-2} yr^{-1})	0.35 ± 0.04	1.4 ± 0.5

Abbreviations: OC, organic carbon; TerrOC, terrigenous OC; TOC, total organic carbon.

account for 44% and 19% of the total variations, respectively. For both the Atacama or Kermadec Trench, the hadal sediments (e.g., A3, A4, A5, A6, K4, and K6) had more negative loadings on the PC1 and were more driven by the TOC/TN and terrigenous/marine biomarker ratios. This suggests that the sediments at the hadal sites were more influenced by terrigenous OC. In contrast, the non-hadal sediments (e.g., A1, A7, A9, and K7) had more positive loadings on the PC1. The sediments from site A1 were more driven by the TOC and TN contents, whereas the sediments from sites K4 and K6 were more related to $\delta^{13}C$, suggesting that their OC was more influenced by marine primary productivity and marine OC source, respectively. Along the PC2, the oceanward abyssal sediments (A7 and K7) always had more negative loadings compared to the hadal sediments (A2, A3, A4, A5, A6, A10, K4, and K6) and landward bathyal/abyssal sediments (A1 and A9), suggesting that PC2 may reflect the strength of terrigenous OC inputs. The samples from cores A3, A4, and A6 were unambiguously separated from those from core A10, even though they are from the same trench axis (Figure 8). These differences highlight the heterogeneity of sediment OC characteristics within the trench interior and the complex nature along the trench axis habitats sustained by the OC supply.

4.4. Estimate of OC Accumulation in the Kermadec and Atacama Trench

There is an imbalance between the estimated riverine OC input (170–200 Tg OC yr^{-1}) and the burial of terrigenous OC in global oceans (58 ± 17 Tg OC yr^{-1}) (Burdige, 2005; Hedges et al., 1997), and the fate of the reminder OC is poorly known. Some studies suggest that the burial of terrigenous OC in the deep sea may be underestimated (Liu et al., 2016; Valier et al., 2007). Indeed, hadal trench systems can represent areas of the enhanced burial of terrigenous OC particularly for those close to large landmasses (Leduc & Rowden, 2018; Xiao et al., 2020). Taking the Atacama Trench (southern part of the Peru-Chile Trench) and Kermadec Trench as examples, we calculated the accumulation rates of total OC and terrigenous OC (g OC m^{-2} yr^{-1}) as:

$$\text{OC accumulation rate} = \text{TOC} \times \text{DBD} \times \text{LSR} \quad (1)$$

$$\text{Terrigenous OC accumulation rate} = \text{OC burial rate}\ F_{terr} \quad (2)$$

where TOC (in weight%) is expressed in g OC per g dry sediment at each sample, DBD is the dry sediment bulk density in g cm^{-3}, LSR is the linear sedimentation rate in cm yr^{-1}, and F_{terr} is the fraction of terrigenous OC in the sediment based on $\delta^{13}C$. The OC accumulation rate is expressed in g m^{-2} yr^{-1}.

This binary mixing model could be applied to cores K6 and A10 which exhibited a non-disturbed continuous deposition of OC as indicated from linear correlations between ^{14}C ages and depths (Figures 2 and 3). The linear regression of ^{14}C ages versus core depth provides an average LSR of 20.1×10^{-3} cm yr^{-1} at site K6 (Kermadec Trench) and of 27.0×10^{-3} cm yr^{-1} at core A10 (Atacama Trench). Although the bioturbation in surface sediments may affect the calculation of sedimentation rates, our estimates based on ^{14}C activity better represent a long-term average rate. An average DBD is 1.49 g cm^{-3} based on previous reports for the New Britain Trench (1.40 g cm^{-3}) (Xiao et al., 2020), Izu-Bonin Trench (1.76 g cm^{-3}), and Tonga Trench (1.32 g cm^{-3}) (Wenzhöfer et al., 2016). The estimated OC accumulation rates according to Equation 1 thus amounts to 0.94 ± 0.08 g m^{-2} yr^{-1} at site K6 (Kermadec Trench) and 5.6 ± 1.4 g m^{-2} yr^{-1} at site A10 (Atacama Trench) (Table 2). These estimated accumulation rates are 6–40 times greater than the average OC accumulation rate of the southern Mariana Trench (0.15 g m^{-2} yr^{-1}) (Luo et al., 2017) but are comparable to the OC accumulation rate of the New Britain Trench (2.8 ± 0.3 g m^{-2} yr^{-1}) (Xiao et al., 2020). It should be noted that these values may underestimate the OC accumulation rates since lateral transport by episodic depositional events to hadal trenches was not considered. Additionally, trench-wide extrapolation of OC accumulation based on a small number of sampling sites can generate large uncertainties and is even problematic considering the highly heterogeneous OC characteristics along the trench axis. However, our conservative estimates reflect a long-term average and should be substantially lower than the OC accumulation

rates during episodic events that contribute enormous amounts of sediment and OC to the hadal trench bottom, as observed at the Japan Trench during the giant 2011 Tohoku-oki earthquake (Kioka et al., 2019).

Given an average value of 1.0 g m^{-2} yr^{-1} for the OC accumulation rate of the global deep ocean (>1,000 m) (Sarmiento & Gruber, 2006), our estimated OC accumulation rate for the Kermadec Trench is almost equivalent to the global average, while the rate for the Atacama Trench is 6-times greater than the global average. Furthermore, given the fractions of terrigenous OC at cores K6 (25%–37%) and A10 (16%–32%), the terrigenous OC accumulation rate was 0.35 ± 0.04 g m^{-2} yr^{-1} at site K6 of the Kermadec Trench and 1.4 ± 0.5 g m^{-2} yr^{-1} at site A10 of the Atacama Trench (Table 2). These estimates are substantially higher than the average of terrigenous OC accumulation rates in the global deep ocean where biomarker and stable isotopic data indicate very little terrigenous OC (Emerson et al., 1987; Hedges et al., 1997). Assuming Kermadec Trench and Atacama Trench are representative of oligo- to mesotrophic and productive hadal trenches, respectively, we extrapolate OC burial rate to the global hadal zone, resulting in a range of 3.8∼22 × 10^{12} g OC yr^{-1} given a total area of 4.0 × 10^{8} km^2 for the hadal zone. Our estimate is close to the literature report based on DSDP and ODP cores surrounding the subduction trenches (12 × 10^{12} g OC yr^{-1}) (Clift, 2017). It is estimated that the annual ocean OC burial is 169 × 10^{12} g (Smith et al., 2015), implying that 2.2%–13% of OC accumulates in the hadal zone. We further calculated the burial rate of terrestrial OC in the hadal zone according to F_{terr} in Kermadec and Atacama trenches, resulting in 1.2∼6.2 × 10^{12} g OC yr^{-1}. This estimate accounts for 2.0%–11% of global ocean terrestrial OC burial (58 × 10^{12} g OC yr^{-1}) (Burdige, 2005). Therefore, the hadal zone is likely an important sink for OC and terrigenous OC in the deep sea.

5. Conclusions

We have conducted a comprehensive study on sedimentary OC characteristics for the Kermadec Trench and Atacama Trench systems. Based on the geochemical data of 12 sediment cores from hadal and non-hadal sites, four conclusions are drawn as following.

(1) Higher sedimentary OC contents were observed in the Atacama Trench as compared to the Kermadec Trench, a difference that can be ascribed to the difference in regional surface ocean productivity. However, extensive heterogeneity of sedimentary OC characteristics was observed, reflected by variable TOC content, TOC/TN ratio, carbon isotopes, and biomarkers within the respective trenches
(2) Hadal sedimentary OC is a mixture of autochthonous marine OC mainly from primary production and allochthonous terrigenous OC mainly derived from adjacent landmasses. The relative enrichment of terrigenous OC along the hadal axes is attributed to efficient lateral transport and/or the preferential preservation of terrigenous OC from biogenic and fossil sources
(3) At the non-hadal sites (abyssal plains/landward slopes), the downcore linear increase in ^{14}C ages and negative shifts of $\delta^{13}C$ suggest a steady accumulation and post-depositional decay of marine-derived OC. Whereas at the hadal sites (trench axes), the reversals in ^{14}C-ages in depth profiles and large changes in TOC contents, TOC/TN ratios, $\delta^{13}C$, and biomarkers suggest unstable depositional conditions truncated by episodic mass-wasting events with variable contributions from mixed terrigenous (older ^{14}C age) and marine-derived (younger ^{14}C age) OC
(4) Significant amounts of total and terrigenous OC are buried along the Kermadec and Atacama trench axes. We thus propose that the hadal zone may be an important terrigenous carbon sink in the deep ocean. Future research that aims at the separation of terrigenous biogenic and fossil OC would allow for assessing the importance of hadal trenches for carbon sequestration in the deep ocean

Data Availability Statement

The data set for this study are available at https://dx.doi.org/10.6084/m9.figshare.13311464.

Acknowledgments
Samples were collected during cruises on the RV SONNE, cruise SO261 (ship time provide by BMBF, Germany) and RV Tangaroa, cruise TAN1711. The authors thank captain(s), the crew(s), and colleagues (Mathias Zabel, Pei-Chuan Chuang, and Emmanuel Okuma) for their excellent support to obtain these samples. Anni Glud is thanked for excellent technical assistance during core slicing and handling of samples. The voyages were made possible by the HADES-ERC Advanced grant "Benthic diagenesis and microbiology of hadal trenches" (grant agreement number 669947) awarded to RN Glud (University of Southern Denmark) (both SO261 and TAN1711), and funding from the Coasts & Oceans Center of New Zealand's National Institute of Water & Atmospheric Research (TAN1711), the Danish Center for Hadal Research via the Danish National Research Foundation (grant DNRF145), National Natural Science Foundation of China (41976030; 41806085; 42076029; 91851210; 91951210; 41773069; 41776064), State Key Laboratory of Marine Geology, Tongji University (No. MGK202003), the State Key R&D project of China (2018YFA0605800, 2018YFC0310600), Shenzhen international collaborative research project (GJHZ20180928155004783), Shenzhen Key Laboratory of Marine Archaea Geo-Omics, Southern University of Science and Technology (ZDSYS20180208184349083). Dr. Philip A. Meyers and Dr. Andrew W. Dale are thanked for their constructive comments.

References

Bao, R., Strasser, M., McNichol, A. P., Haghipour, N., McIntyre, C., Wefer, G., et al. (2018). Tectonically-triggered sediment and carbon export to the Hadal zone. *Nature Communications*, *9*. https://doi.org/10.1038/s41467-017-02504-1

Baudin, F., Martinez, P., Dennielou, B., Charlier, K., Marsset, T., Droz, L., & Rabouille, C. (2017). Organic carbon accumulation in modern sediments of the Angola basin influenced by the Congo deep-sea fan. *Deep Sea Research Part II: Topical Studies in Oceanography*, *142*, 64–74. https://doi.org/10.1016/j.dsr2.2017.01.009

Behrenfeld, M. J., & Falkowski, P. G. (1997). Photosynthetic rates derived from satellite-based chlorophyll concentration. *Limnology & Oceanography*, *42*, 1–20. https://doi.org/10.4319/lo.1997.42.1.0001

Brodowski, S., Rodionov, A., Haumaier, L., Glaser, B., & Amelung, W. (2005). Revised black carbon assessment using benzene polycarboxylic acids. *Organic Geochemistry*, *36*, 1299–1310. https://doi.org/10.1016/j.orggeochem.2005.03.011

Burdige, D. J. (2005). Burial of terrestrial organic matter in marine sediments: A re-assessment. *Global Biogeochemical Cycles*, *19*. https://doi.org/10.1029/2004GB002368

Burdige, D. J. (2007). Preservation of organic matter in marine sediments: Controls, mechanisms, and an imbalance in sediment organic carbon budgets? *Chemical Reviews*, *107*, 467–485. https://doi.org/10.1021/cr050347q

Clift, P. D. (2017). A revised budget for Cenozoic sedimentary carbon subduction. *Reviews of Geophysics*, *55*, 97–125. https://doi.org/10.1002/2016rg000531

Danovaro, R., Della Croce, N., Dell'Anno, A., & Pusceddu, A. (2003). A depocenter of organic matter at 7800m depth in the SE Pacific Ocean. *Deep Sea Research Part I: Oceanographic Research Papers*, *50*, 1411–1420. https://doi.org/10.1016/j.dsr.2003.07.001

Danovaro, R., Gambi, C., & Della Croce, N. (2002). Meiofauna hotspot in the Atacama Trench, eastern South Pacific Ocean. *Deep Sea Research Part I: Oceanographic Research Papers*, *49*, 843–857. https://doi.org/10.1016/S0967-0637(01)00084-X

de Stigter, H. C., Boer, W., de Jesus Mendes, P. A., Jesus, C. C., Thomsen, L., van den Bergh, G. D., & van Weering, T. C. E. (2007). Recent sediment transport and deposition in the Nazaré Canyon, Portuguese continental margin. *Marine Geology*, *246*, 144–164. https://doi.org/10.1016/j.margeo.2007.04.011

Dickens, A. F., Gélinas, Y., Masiello, C. A., Wakeham, S., & Hedges, J. I. (2004). Reburial of fossil organic carbon in marine sediments. *Nature*, *427*, 336–339. https://doi.org/10.1038/nature02299

Eglinton, T. I., Benitez-Nelson, B., Pearson, A., McNichol, A., Bauer, J. E., & Druffel, E. (1997). Variability in radiocarbon ages of individual organic compounds from marine sediments. *Science*, *277*, 796–799. https://doi.org/10.1126/science.277.5327.796

Emerson, S., Stump, C., Grootes, P. M., Stuiver, M., Farwell, G. W., & Schmidt, F. H. (1987). Estimates of degradable organic carbon in deep-sea surface sediments from 14C concentrations. *Nature*, *329*, 51–53. https://doi.org/10.1038/329051a0

French, K. L., Hein, C. J., Haghipour, N., Wacker, L., Kudrass, H. R., Eglinton, T. I., et al. (2018). Millennial soil retention of terrestrial organic matter deposited in the Bengal fan. *Scientific Reports*, *8*. https://doi.org/10.1038/s41598-018-30091-8

Gallo, N. D., James, C., Kevin, H., Patricia, F., Douglas, H. B., & Lisa, A. L. (2015). Submersible- and lander-observed community patterns in the Mariana and New Britain trenches: Influence of productivity and depth on epibenthic and scavenging communities. *Deep Sea Research Part I: Oceanographic Research Papers*, *99*, 119–133. https://doi.org/10.1016/j.dsr.2014.12.012

Giovanni, D., Victor, D., Renato, Q. Â. o., Barbara, J., Paulina, M., & Osvaldo, U. (2000). Primary production and community respiration in the Humboldt Current System off Chile and associated oceanic areas. *Marine Ecology Progress Series*, *197*, 41–49. https://doi.org/10.3354/meps197041

Glud, R. N., Berg, P., Thamdrup, B., Larsen, M., Stewart, H. A., Jamieson, A. J., et al. (2021). Hadal trenches are dynamic hotspots for early diagenesis in the deep sea. *Communications Earth & Environment*, *2*, 21. https://doi.org/10.1038/s43247-020-00087-2

Glud, R. N., Wenzhöfer, F., Middelboe, M., Oguri, K., Turnewitsch, R., Canfield, D. E., & Kitazato, H. (2013). High rates of microbial carbon turnover in sediments in the deepest oceanic trench on Earth. *Nature Geoscience*, *6*, 284–288. https://doi.org/10.1038/ngeo1773

Hedges, J. I., Keil, R. G., & Benner, R. (1997). What happens to terrestrial organic matter in the ocean? *Organic Geochemistry*, *27*, 195–212. https://doi.org/10.1016/S0146-6380(97)00066-1

Henrichs, S. M. (1992). Early diagenesis of organic matter in marine sediments: Progress and perplexity. *Marine Chemistry*, *39*, 119–149. https://doi.org/10.1016/0304-4203(92)90098-U

Hu, F. S., Hedges, J. I., Gordon, E. S., & Brubaker, L. B. (1999). Lignin biomarkers and pollen in postglacial sediments of an Alaskan lake. *Geochimica et Cosmochimica Acta*, *63*, 1421–1430. https://doi.org/10.1016/S0016-7037(99)00100-3

Huene, R. v., Weinrebe, W., & Heeren, F. (1999). Subduction erosion along the North Chile margin. *Journal of Geodynamics*, *27*, 345–358. https://doi.org/10.1016/S0264-3707(98)00002-7

Ichino, M. C., Clark, M. R., Drazen, J. C., Jamieson, A., Jones, D. O. B., Martin, A. P., et al. (2015). The distribution of benthic biomass in hadal trenches: A modeling approach to investigate the effect of vertical and lateral organic matter transport to the seafloor. *Deep Sea Research Part I: Oceanographic Research Papers*, *100*, 21–33. https://doi.org/10.1016/j.dsr.2015.01.010

Itoh, M., Kawamura, K., Kitahashi, T., Kojima, S., Katagiri, H., & Shimanaga, M. (2011). Bathymetric patterns of meiofaunal abundance and biomass associated with the Kuril and Ryukyu trenches, western North Pacific Ocean. *Deep Sea Research Part I: Oceanographic Research Papers*, *58*, 86–97. https://doi.org/10.1016/j.dsr.2010.12.004

Itou, M., Matsumura, I., & Noriki, S. (2000). A large flux of particulate matter in the deep Japan Trench observed just after the 1994 Sanriku-Oki earthquake. *Deep Sea Research Part I: Oceanographic Research Papers*, *47*, 1987–1998. https://doi.org/10.1016/S0967-0637(00)00012-1

Jamieson, A. (2015). *The hadal zone: Life in the deepest oceans*. Cambridge University Press. https://doi.org/10.1017/cbo9781139061384

Kioka, A., Schwestermann, T., Moernaut, J., Ikehara, K., Kanamatsu, T., McHugh, C. M., et al. (2019). Megathrust earthquake drives drastic organic carbon supply to the hadal trench. *Scientific Reports*, *9*. https://doi.org/10.1038/s41598-019-38834-x

Leduc, D., & Rowden, A. A. (2018). Not to be sneezed at: Does pollen from forests of exotic pine affect deep oceanic trench ecosystems? *Ecosystems*, *21*, 237–247. https://doi.org/10.1007/s10021-017-0146-8

Leithold, E. L., Blair, N. E., & Perkey, D. W. (2006). Geomorphologic controls on the age of particulate organic carbon from small mountainous and upland rivers. *Global Biogeochemical Cycles*, *20*, GB3022. https://doi.org/10.1029/2005gb002677

Li, D., Zhao, J., Yao, P., Liu, C., Sun, C., Chen, J., et al. (2020). Spatial heterogeneity of organic carbon cycling in sediments of the northern Yap Trench: Implications for organic carbon burial. *Marine Chemistry*, *223*, 103813. https://doi.org/10.1016/j.marchem.2020.103813

Liu, J. T., Hsu, R. T., Hung, J.-J., Chang, Y.-P., Wang, Y.-H., Rendle-Bühring, R. H., et al. (2016). From the highest to the deepest: The Gaoping River-Gaoping Submarine Canyon dispersal system. *Earth-Science Reviews*, *153*, 274–300. https://doi.org/10.1016/j.earscirev.2015.10.012

Liu, J. T., Kao, S.-J., Huh, C.-A., & Hung, C.-C. (2013). Gravity flows associated with flood events and carbon burial: Taiwan as instructional source area. *Annual Review of Marine Science*, *5*, 47–68. https://doi.org/10.1146/annurev-marine-121211-172307

Luo, M., Gieskes, J., Chen, L., Scholten, J., Pan, B., Lin, G., & Chen, D. (2019). Sources, Degradation, and Transport of Organic Matter in the New Britain Shelf-Trench Continuum, Papua New Guinea. *Journal of Geophysical Research: Biogeosciences*, *124*, 1680–1695. https://doi.org/10.1029/2018jg004691

Luo, M., Gieskes, J., Chen, L., Shi, X., & Chen, D. (2017). Provenances, distribution, and accumulation of organic matter in the southern Mariana Trench rim and slope: Implication for carbon cycle and burial in hadal trenches. *Marine Geology*, *386*, 98–106. https://doi.org/10.1016/j.margeo.2017.02.012

Meyers, P. A. (1997). Organic geochemical proxies of paleoceanographic, paleolimnologic, and paleoclimatic processes. *Organic Geochemistry*, *27*, 213–250. https://doi.org/10.1016/S0146-6380(97)00049-1

Niggemann, J., Ferdelman, T. G., Lomstein, B. A., Kallmeyer, J., & Schubert, C. J. (2007). How depositional conditions control input, composition, and degradation of organic matter in sediments from the Chilean coastal upwelling region. *Geochimica et Cosmochimica Acta*, *71*, 1513–1527. https://doi.org/10.1016/j.gca.2006.12.012

Oguri, K., Kawamura, K., Sakaguchi, A., Toyofuku, T., Kasaya, T., Murayama, M., et al. (2013). Hadal disturbance in the Japan Trench induced by the 2011 Tohoku–Oki earthquake. *Scientific Reports*, *3*. https://doi.org/10.1038/srep01915

Pancost, R. D., & Boot, C. S. (2004). The paleoclimatic utility of terrestrial biomarkers in marine sediments. *Marine Chemistry*, *92*, 239–261. https://doi.org/10.1016/j.marchem.2004.06.029

Pancost, R. D., Freeman, K. H., & Wakeham, S. G. (1999). Controls on the carbon-isotope compositions of compounds in Peru surface waters. *Organic Geochemistry*, *30*, 319–340. https://doi.org/10.1016/S0146-6380(99)00004-2

Perdue, E. M., & Koprivnjak, J.-F. (2007). Using the C/N ratio to estimate terrigenous inputs of organic matter to aquatic environments. *Estuarine, Coastal and Shelf Science*, *73*, 65–72. https://doi.org/10.1016/j.ecss.2006.12.021

Popp, B. N., Trull, T., Kenig, F., Wakeham, S. G., Rust, T. M., Tilbrook, B., et al. (1999). Controls on the carbon isotopic composition of Southern Ocean phytoplankton. *Global Biogeochemical Cycles*, *13*, 827–843. https://doi.org/10.1029/1999gb900041

Prahl, F. G., De Lange, G. J., Scholten, S., & Cowie, G. L. (1997). A case of post-depositional aerobic degradation of terrestrial organic matter in turbidite deposits from the Madeira Abyssal Plain. *Organic Geochemistry*, *27*, 141–152. https://doi.org/10.1016/S0146-6380(97)00078-8

Reimer, P. J., Bard, E., Bayliss, A., Beck, J. W., Blackwell, P. G., Ramsey, C. B., et al. (2013). IntCal13 and Marine13 Radiocarbon Age Calibration Curves 0-50,000 Years cal BP. *Radiocarbon*, *55*, 1869–1887. https://doi.org/10.2458/azu_js_rc.55.16947

Richardson, M. D., Briggs, K. B., Bowles, F. A., & Tietjen, J. H. (1995). A depauperate benthic assemblage from the nutrient-poor sediments of the Puerto Rico Trench. *Deep Sea Research Part I: Oceanographic Research Papers*, *42*, 351–364. https://doi.org/10.1016/0967-0637(95)00007-S

Sarmiento, J. L., & Gruber, N. (2006). *Ocean biogeochemical dynamics*. Princeton, USA: Princeton University Press.

Smith, R. W., Bianchi, T. S., Allison, M., Savage, C., & Galy, V. (2015). High rates of organic carbon burial in fjord sediments globally. *Nature Geoscience*, *8*, 450–453. https://doi.org/10.1038/ngeo2421

Stewart, H. A., & Jamieson, A. J. (2018). Habitat heterogeneity of hadal trenches: Considerations and implications for future studies. *Progress in Oceanography*, *161*, 47–65. https://doi.org/10.1016/j.pocean.2018.01.007

Sutton, P., Chiswell, S., Gorman, R., Kennan, S., & Rickard, G. (2012). Physical marine environment of the Kermadec Islands region, in *Science for conservation*, (pp. 1–16), Department of Conservation, Wellington.

Trumbore, S. (2009). Radiocarbon and Soil Carbon Dynamics. *Annual Review of Earth and Planetary Sciences*, *37*, 47–66. https://doi.org/10.1146/annurev.earth.36.031207.124300

Turnewitsch, R., Falahat, S., Stehlikova, J., Oguri, K., Glud, R. N., Middelboe, M., et al. (2014). Recent sediment dynamics in hadal trenches: Evidence for the influence of higher-frequency (tidal, near-inertial) fluid dynamics. *Deep Sea Research Part I: Oceanographic Research Papers*, *90*, 125–138. https://doi.org/10.1016/j.dsr.2014.05.005

Valier, G., Bernhard, P. E., & Timothy, E. (2015). Global carbon export from the terrestrial biosphere controlled by erosion. *Nature*, *521*, 204–207. https://doi.org/10.1038/nature14400

Valier, G., Christian, F. L., Olivier, B., Pierre, F., Hermann, K., & Fabien, P. (2007). Efficient organic carbon burial in the Bengal fan sustained by the Himalayan erosional system. *Nature*, *450*, 407–410. https://doi.org/10.1038/nature06273

Vargas, C., Arriagada, L., Sobarzo, M., Contreras, P., & Saldías, G. (2013). Bacterial production along a river-to-ocean continuum in central Chile: Implications for organic matter cycling. *Aquatic Microbial Ecology*, *68*, 195–213. https://doi.org/10.1002/2015JG003213

Volkman, J. K. (2006). *Marine organic matter: Biomarkers, isotopes and DNA*. Berlin, Heidelberg: Springer. https://doi.org/10.1007/b11682

Volkman, J. K., Barrett, S. M., Blackburn, S. I., Mansour, M. P., Sikes, E. L., & Gelin, F. (1998). Microalgal biomarkers: A review of recent research developments. *Organic Geochemistry*, *29*, 1163–1179. https://doi.org/10.1016/S0146-6380(98)00062-X

Wenzhöfer, F., Oguri, K., Middelboe, M., Turnewitsch, R., Toyofuku, T., Kitazato, H., & Glud, R. N. (2016). Benthic carbon mineralization in hadal trenches: Assessment by in situ O2 microprofile measurements. *Deep Sea Research Part I: Oceanographic Research Papers*, *116*, 276–286. https://doi.org/10.1016/j.dsr.2016.08.013

Xiao, W., Xu, Y., Haghipour, N., Montluçon, D. B., Pan, B., Jia, Z., et al. (2020). Efficient sequestration of terrigenous organic carbon in the New Britain Trench. *Chemical Geology*, *533*. https://doi.org/10.1016/j.chemgeo.2019.119446

Xu, X., Trumbore, S. E., Zheng, S., Southon, J. R., McDuffee, K. E., Luttgen, M., & Liu, J. C. (2007). Modifying a sealed tube zinc reduction method for preparation of AMS graphite targets: Reducing background and attaining high precision. *Nuclear Instruments and Methods in Physics Research Section B: Beam Interactions with Materials and Atoms*, *259*, 320–329. https://doi.org/10.1016/j.nimb.2007.01.175

Xu, Y., Jia, Z., Xiao, W., Fang, J., Wang, Y., Luo, M., et al. (2020). Glycerol dialkyl glycerol tetraethers in surface sediments from three Pacific trenches: Distribution, source and environmental implications. *Organic Geochemistry*, *147*, 104079. https://doi.org/10.1016/j.orggeochem.2020.104079

Xu, Y., Zhou, S., Hu, L., Wang, Y., & Xiao, W. (2018). Different controls on sedimentary organic carbon in the Bohai Sea: River mouth relocation, turbidity and eutrophication. *Journal of Marine Systems*, *180*, 1–8. https://doi.org/10.1016/j.jmarsys.2017.12.004